Outage Analysis of Underlaid Multi-Antenna D2D Communication in Cellular Networks

Nilupuli Senadhira, Jing Guo and Salman Durrani
Research School of Engineering, The Australian National University, Canberra, ACT 2601, Australia.
Corresponding author email: jing.guo@anu.edu.au.

***Abstract*—In this work, we consider in-band device-to-device (D2D) communication underlaid with an uplink cellular network, where D2D users are equipped with multiple antennas. We assume that the D2D users employ the distance cut-off mode selection scheme to reduce the interference to base stations. With the help of stochastic geometry, we derive the approximate yet accurate analytical outage probability experienced at the base station and the D2D receiver. The accuracy of the derived analytical results is confirmed by simulation results. Our numerical results show that having multi-antenna D2D users can improve the outage probability at the D2D receiver, while the outage probability at the base station is not impacted. In addition, equal number of D2D transmit and receive antennas can provide better D2D receiver outage performance. The results also show that a smaller value of the distance cut-off threshold is a good choice as it achieves good D2D communication and does not adversely impact the cellular network performance.**

***Index Terms*—Device-to-device communication, stochastic geometry, multiple antennas, mode selection.**

I. Introduction

Device-to-device (D2D) communication, allowing devices located in close proximity to directly communicate with each other without going through the base station (BS), is envisaged as a key technology for fifth generation (5G) cellular networks [1–3]. In underlay in-band D2D communication, the devices are allowed to concurrently utilize the resources for cellular users, which improves the spectral efficiency. However, it also causes the intra-cell and inter-cell interference because of the spectral reuse [4]. Hence, mode selection schemes are used to limit the interference to the base stations [4–6].

The interference modelling and management in D2D communication have been investigated in the literature using stochastic geometry [4–10]. As a powerful mathematical tool, stochastic geometry allows the tractable computation of the performance metrics while capturing the randomness in the locations of the devices. However, most of the prior work in the literature assumed nodes employing single antennas only. Multiple antennas are expected to play an important role in future 5G wireless communication networks. It is well known that the use of multiple antennas can reduce the interference and improve the capacity of the network as it exploits the diversity provided by fading channels. Therefore, D2D enabled wireless networks where D2D users are equipped with multiple antennas is an important research topic.

The performance analysis of traditional cellular networks with multiple antennas has been well studied in the literature using stochastic geometry [11–14]. Recently, some papers have considered multiple antennas with D2D communication [15–19]. Specifically, both [15] and [16] assumed multiple antennas at the BS side, where an interference limited area control scheme was proposed in [15] and [16] studied the mode selection schemes. The rate maximization problems for both cellular and D2D communication were studied in [17]. However, [15–17] considered the fixed location for users, while in practice, the location of users can be random. Although [18] and [19] studied the multiple antenna systems in D2D communication using stochastic geometry, they did not incorporate any D2D mode selection scheme to manage the interference. Note that, in general, the consideration of multiple antennas makes the application of stochastic geometry more complicated and technically challenging [20].

In this paper, we extend the results in [6, 11] and employ the stochastic geometry to study the performance of the D2D communication underlaid with the uplink cellular network. We assume that the cellular users and base stations are equipped with single omnidirectional antennas, while the D2D users are equipped with multiple antennas. We adopt the distance cut-off mode selection scheme [4] for D2D users to reduce the interference to the base stations. Using the outage probability as the performance metric, we investigate the impact of the multi-antenna D2D users on the cellular uplink and D2D communication. In particular, we investigate and compare the scenarios where the D2D transmitter and receiver pairs form either single-input multiple-output (SIMO) systems or MIMO systems. We also examine the impact of the D2D mode selection scheme. The major contributions of this paper are:

- Using stochastic geometry, we analytically compute the outage probability experienced at the base station and the D2D receiver. In particular, by assuming that D2D transmitters have M_t antennas and D2D receivers have M_r antennas, we provide a general analytical formulation for the outage probability at the D2D receiver (Theorem 2). We provide closed-form results for two special cases when the D2D transmitter and receiver pairs form either $1 \times M_r$ SIMO systems or 2×2 MIMO systems. We verify the accuracy of our derived analytical results by comparing with the simulation results.
- Using our analytical results, we investigate the impact of multi-antenna D2D communication in an underlay uplink cellular network. Our results show that having multi-antenna D2D users improves the outage probability at

978-1-5090-0941-1/16/$31.00 ©2016 IEEE

the D2D receiver, while the outage probability at the base station is not impacted. In addition, equal number of D2D transmit and receive antennas provides better D2D receiver outage performance.
- Our results also show that with multi-antenna D2D users, a smaller value of the distance cut-off threshold parameter is a good choice. This is because only closely located multi-antenna D2D users are allowed to communicate, which generates less interference and does not adversely impact the cellular network performance.

The rest of the paper is organised as follows. The system model is presented in Section II. The analytical results are derived in Section III. The simulation results are presented and discussed in Section IV. Finally, conclusions are presented in Section V.

The following notation is used in the paper. $\Pr(\cdot)$ is the probability measure and $E[\cdot]$ denotes the expectation operator. $\exp(\cdot)$ is the exponential function. $\Gamma(\cdot)$ is the complete gamma function while $\gamma(\cdot,\cdot)$ denotes the lower incomplete gamma function. ${}_2F_1(\cdot,\cdot;\cdot;\cdot)$ is the hypergeometric function. $I_{\text{CUE}}^{\text{BS}}$ denotes the aggregate interference from cellular users equipments (CUEs) to the BS, and $I_{\text{DTX}}^{\text{BS}}$ is the aggregate interference from D2D transmitters (DTXs) to the base stations (BS). Similarly, $I_{\text{CUE}}^{\text{DRX}}$ and $I_{\text{DTX}}^{\text{DRX}}$ represent the aggregate interference from cellular users to the D2D receiver (DRX) and the aggregate interference from D2D transmitters to the D2D receiver, respectively. Moreover, the subscripts 0, c and d denote the desired link, cellular links and D2D links, respectively.

II. System Model

Consider a D2D-enabled single (macro) tier network, where the base stations are placed according to a hexagonal grid. The density of BSs is given by λ_b, such that the area of the hexagonal cell is $\frac{1}{\lambda_b}$ (i.e., each hexagonal cell has only one BS located at the center of the hexagonal cell). Generally the shape of a hexagonal cell can be approximated as a disk with radius R, where the radius is related to the density of BSs by $\frac{1}{\lambda_b} = \frac{3\sqrt{3}}{2}R^2$ [4].

The network consists of two types of transmitters, namely cellular user equipments (CUEs) and potential D2D transmitters (DTXs). The locations of the CUEs and the potential DTXs are modelled as the independent homogeneous Poisson point processes (PPPs), ϕ_c with density λ_c and ϕ_d with density λ_d, respectively. We further assume that each potential DTX has an intended D2D receiver (DRX) at a distance r_d in a random direction. Note that a potential DTX can be either in D2D mode (i.e., it bypasses the BS and communicates directly with the intended DRX) or in the other transmission mode according to the mode selection scheme. In this work, we employ the distance cut-off mode selection scheme [4]. According to this scheme, the D2D link distance r_d is compared with a cut-off parameter β. If $r_d < \beta$, the DTX-DRX pair is active. Otherwise, the potential DTX goes into outage (i.e., it keeps silent) [6].

We consider the uplink transmission scenario, where the CUE is always associated to its closest BS. We also assume that $\lambda_c \gg \lambda_b$ such that each BS has at least one associated CUE. Multiple CUEs in a macrocell are scheduled to access the licensed channel using a round-robin fashion, which implies that only one CUE is occupying the available channel in a macrocell. Hence, the CUEs are not subjected to intra-cell interference. The underlay in-band D2D communication is considered in this work where all the DTXs share the same channel with the CUEs.

A. Link Distances

Inside a macrocell, the CUE can be regarded as randomly and uniformly distributed. Hence, the probability density function (pdf) of the distance of the CUE from the BS (cellular link distance) is given by [6]

$$f_{r_c}(r_c) = \frac{2r_c}{R^2}, \qquad 0 \le r_c \le R. \tag{1}$$

The random distance between the DTX and DRX can be modelled by a normalised Rayleigh distribution with pdf given by [6]

$$f_{r_d}(r_d) = \frac{2\pi r_d \lambda_d \exp(-\pi\lambda_d r_d^2)}{1-\exp(-\pi\lambda_d R_{\max}^2)}, \qquad 0 \le r_d \le R_{\max}. \tag{2}$$

B. Channel Model and Power Control

The communication channel is modelled by a path loss plus Rayleigh fading. Note that Rayleigh fading can be viewed as an independent and identically distributed complex Gaussian random variable. For the path loss model, the average transmit signal power decays at the rate of $r^{-\eta}$, where r and η refer to the link distance and the path loss exponent, respectively. Two different path loss exponents, η_c and η_d are considered as different propagation environments can be experienced by the cellular and the D2D links.

Additionally, both CUEs and DTXs use full channel inversion power control [4]. Under such a scheme, the average received power at the intended receiver (BS or DRX) is maintained at a threshold ρ by compensating the path loss (i.e., the transmit power will be ρr^{η}). Moreover, we assume that there is a maximum transmit power constraint P_u for the D2D users. Hence, the D2D proximity is given by $R_{\max} = \left(\frac{P_u}{\rho}\right)^{\frac{1}{\eta_d}}$.

C. Multiple-Input Multiple-Output (MIMO) Beamforming

The CUEs and BS are assumed to be equipped with single omnidirectional antennas, while DTXs and DRXs have M_t and M_r number of antennas, respectively.[1] We adopt the MIMO eigen-beamforming technique, in which the DTX sends the linearly weighted versions of the signal on each antenna and the DRX receives a coherent linear combination of the antenna outputs [11]. We assume that all the DTXs and DRXs have the perfect channel state information only for their own channel but not the interfering channels. As a result, the signalling strategy becomes the maximization of the desired received signal power [11].

[1]Note that our framework can be extended to study the case where BSs and CUEs also have multiple antennas. This is outside the scope of the present work and can be considered in future work.

III. Analytical Framework

In this section we discuss the general analytical framework to study the outage probability at the BS and the DRx. Because of the concurrent transmission, DTXs cause interference to the BS and other DRXs, while CUEs cause interference to other BSs and DRXs. Since the network is interference limited, we neglect the thermal noise when analyzing the outage probability [11]. The outage probability is, therefore, defined as the average probability that the SIR at the typical RX (BS or DRX) is less than a certain SIR threshold θ.

Before studying the outage probability, we present some preliminaries which help to derive the outage probability.

A. Preliminary Results

The potential DTXs can be in either D2D mode or silent mode. Only the potential DTXs in D2D mode will generate the interference. Hence, in the following, we show the probability of being in D2D mode for a potential DTX.

Lemma 1. *In the distance-cut off mode selection scheme, D2D mode is selected by the potential DTXs if the condition $r_d < \beta$ is satisfied. The probability of being in D2D mode for a potential DTX is given by [4, 6]*

$$P_{\mathrm{D2D}} = \frac{1-\exp\left(-\pi\lambda_d\beta^2\right)}{1-\exp\left(-\pi\lambda_d R_{\max}^2\right)}, \tag{3}$$

where β is the cut-off parameter.

As the transmit power for both CUE and DTX is not constant but depends on the distance to their desired receiver, the following lemmas show the α-th moment of the corresponding transmit power.

Lemma 2. *For a CUE, the α-th moment of the cellular transmit power P_c is given by*

$$E_{P_c}[P_c^{\alpha}] = \frac{2\rho^{\alpha}R^{\alpha\eta_c}}{\alpha\eta_c+2}. \tag{4}$$

Lemma 3. *For a DTX, the α-th moment of the D2D transmit power P_d is given by*

$$E_{P_d}[P_d^{\alpha}] = \frac{(\pi\lambda_d)^{-\frac{\alpha\eta_d}{2}}\rho^{\alpha}}{1-\exp(-\pi\lambda_d\beta^2)}\gamma\left(\frac{\alpha\eta_d}{2}+1, \pi\lambda_d\beta^2\right). \tag{5}$$

Proof: The instantaneous transmit power for a CUE and DTX are given by $P_c = \rho r_c^{\eta_c}$ and $P_d = \rho r_d'^{\eta_c}$, respectively. Note that r_d' is the distance given that the potential DTX is in D2D mode and its distribution is given by $f_{r_d'}(r_d') = \frac{2\pi r_d'\lambda_d\exp(-\pi\lambda_d(r_d')^2)}{1-\exp(-\pi\lambda_d\beta^2)}$, $0 \le r_d' \le \beta$. After averaging the instantaneous power with respect to the distribution of r_c (or r_d'), we obtain the above results. ∎

B. Outage Probability at the BS

Let the typical BS be located at the origin and a generic CUE is attached to it. The instantaneous signal-to-interference ratio (SIR) at the typical BS can be expressed as

$$SIR^{\mathrm{BS}} = \frac{\rho g_0^{\mathrm{BS}}}{I_{\mathrm{CUE}}^{\mathrm{BS}} + I_{\mathrm{DTX}}^{\mathrm{BS}}}, \tag{6}$$

where $I_{\mathrm{CUE}}^{\mathrm{BS}} = \sum_{x_i\in\phi_c'} P_{ci}|x_i|^{-\eta_c}g_i^{\mathrm{BS}}$ and $I_{\mathrm{DTX}}^{\mathrm{BS}} = \sum_{y_j\in\phi_d'} P_{dj}|y_j|^{-\eta_c}h_j^{\mathrm{BS}}$ represent the aggregate interference caused by the CUEs and DTXs, respectively, ϕ_c' and ϕ_d' are the point process of the interfering CUEs and DTXs, x_i denotes both the i-th interfering CUE and its location, y_j denotes both the j-th interfering DTX and its location, $|x_i|$ and $|y_j|$ are their distance to the typical BS, g_0^{BS} is the fading gain on the desired link between the generic CUE and typical BS, g_i^{BS} is the fading gain between the i-th interfering CUE and typical BS and h_j^{BS} is the fading gain between the j-th interfering DTX and the typical BS.

Both g_0^{BS} and g_i^{BS} follow the exponential distribution, respectively, since we consider a single antenna at the BS and the CUE. Based on the MIMO eigen-beamforming technique and Rayleigh fading assumption, h_j^{BS} also follows the exponential distribution regardless of the number of antennas at the interfering DTX [11].

We can express the outage probability at the BS as

$$P_{\mathrm{out}}^{\mathrm{BS}} = \Pr(SIR^{\mathrm{BS}} \le \theta) = \Pr\left(\frac{\rho g_0^{\mathrm{BS}}}{I_{\mathrm{CUE}}^{\mathrm{BS}} + I_{\mathrm{DTX}}^{\mathrm{BS}}} \le \theta\right). \tag{7}$$

Using the stochastic geometry, we obtain the closed-form outage probability at the BS in the following theorem.

Theorem 1. *For a D2D-enabled single tier cellular network operating under the distance cut-off mode selection scheme, where CUEs and DTXs use full channel inversion power control, the BSs and CUEs are equipped with single antennas while DTXs have M_t antennas and DRXs have M_r antennas, the outage probability experienced at a typical BS for a generic CUE is given by*

$$\begin{aligned} P_{\mathrm{out}}^{\mathrm{BS}} = 1 - \exp\Bigg(&\frac{\pi\lambda_b R^2\theta}{(2-\eta_c)(2+\eta_c)}\Big((2+\eta_c) \\ &\times {}_2F_1\left(1, 1-\frac{2}{\eta_c}; 2-\frac{2}{\eta_c}; -\theta\right) + (2-\eta_c) \\ &\times {}_2F_1\left(1, 1+\frac{2}{\eta_c}; 2+\frac{2}{\eta_c}; -\theta\right)\Big) - \pi\frac{(\pi\lambda_d)^{-\frac{\eta_d}{\eta_c}}\lambda_d\theta^{\frac{2}{\eta_c}}}{1-\exp(-\pi\lambda_d R_{\max}^2)} \\ &\times \gamma\left(\frac{\eta_d}{\eta_c}+1, \pi\lambda_d\beta^2\right)\Gamma\left(1+\frac{2}{\eta_c}\right)\Gamma\left(1-\frac{2}{\eta_c}\right) - \frac{\theta}{\rho}\Bigg). \end{aligned} \tag{8}$$

Proof: See Appendix A. ∎

Remark 1. The result in Theorem 1 is the same as the result in [6], where all BSs, CUEs and D2D users were assumed to be equipped with single antennas. This is because, as discussed below (6), the fading gain between the interfering multi-antenna DTX and the typical BS follows the exponential distribution. Hence, the outage probability at the BS is not impacted when the D2D users are equipped with multiple antennas. We have included a more detailed proof of Theorem 1 in Appendix A since similar steps are needed to derive other results in the paper.

C. Outage Probability at the DRX

In order to characterize the outage probability at the DRX, we condition on the typical DRX being located at the origin. According to Slivnyak's theorem, adding a point in a PPP does not change the distribution of the rest of the process [21]. Similar to the case of the outage probability at the BS, we can express the outage probability at the DRX as

$$P_{\text{out}}^{\text{DRX}} = \Pr(SIR^{\text{D2D}} \leq \theta) = \Pr\left(\frac{\rho g_0^{\text{DRX}}}{I_{\text{CUE}}^{\text{DRX}} + I_{\text{DTX}}^{\text{DRX}}} \leq \theta\right), \quad (9)$$

where $I_{\text{CUE}}^{\text{DRX}} = \sum_{x_i \in \phi'_c} P_{ci}|x_i|^{-\eta_d} g_i^{\text{DRX}}$ and $I_{\text{DTX}}^{\text{DRX}} = \sum_{y_j \in \phi'_d} P_{dj}|y_j|^{-\eta_d} h_j^{\text{DRX}}$ represent the aggregate interference caused by the CUEs and DTXs, respectively, g_i^{DRX} denotes the fading gain between the i-th interfering CUE and the typical DRX and h_j^{DRX} denotes the fading gain between the j-th interfering DTX and the typical DRX.

Again, from the MIMO eigen-beamforming technique and Rayleigh fading assumption, both g_i^{DRX} and h_j^{DRX} follow the identical and independent exponential distribution [11]. With regards to the fading gain on the desired link between the typical DTX and the typical DRX, g_0^{DRX}, its distribution is much more complicated and depends on the number of antennas M_t and M_r. It is given by (23) in Appendix B. A detailed discussion is provided in Appendix B.

Using the stochastic geometry, we can obtain the outage probability at the DRX. First we present two Lemmas, which help to express the final result presented in Theorem 2.

Lemma 4. *The Laplace transform of the pdf of the random sum of cellular interference in the D2D link, $\mathcal{L}_{I_{\text{CUE}}^{\text{DRX}}}(s)$, is*

$$\mathcal{L}_{I_{\text{CUE}}^{\text{DRX}}}(s) = \exp\left(\frac{-2\pi\lambda_b}{\eta_d} E_{P_c}\left[P_c^{\frac{2}{\eta_d}}\right] s^{\frac{2}{\eta_d}} \Gamma\left(\frac{2}{\eta_d}\right)\Gamma\left(1 - \frac{2}{\eta_d}\right)\right). \quad (10)$$

Proof: The proof is similar to the derivation of $\mathcal{L}_{I_{\text{CUE}}^{\text{BS}}}(s)$ in Theorem 1 (presented in Appendix A), except that the integral for the distance between the interfering CUE and the typical DRX becomes $[0, \infty]$ and not $[R, \infty]$. The detailed steps are omitted here for the sake of brevity. ■

Lemma 5. *The Laplace transform of the pdf of the random sum of D2D interference in the D2D link, $\mathcal{L}_{I_{\text{DTX}}^{\text{DRX}}}(s)$, is*

$$\mathcal{L}_{I_{\text{DTX}}^{\text{DRX}}}(s) = \exp\left(\frac{-2\pi P_{\text{D2D}}\lambda_d}{\eta_d} E_{P_d}\left[P_d^{\frac{2}{\eta_d}}\right] s^{\frac{2}{\eta_d}} \times \Gamma\left(\frac{2}{\eta_d}\right)\Gamma\left(1 - \frac{2}{\eta_d}\right)\right). \quad (11)$$

Proof: The proof is similar to the derivation of $\mathcal{L}_{I_{\text{DTX}}^{\text{BS}}}(s)$ in Theorem 1 (presented in Appendix A) and is omitted here for the sake of brevity. ■

Theorem 2. *For a D2D-enabled single tier cellular network operating under the distance cut-off mode selection scheme, where CUEs and DTXs use full channel inversion power control, the BSs and CUEs are equipped with single antennas while DTXs have M_t antennas and DRXs have M_r antennas, the outage probability experienced at a typical DRX is given by*

$$P_{\text{out}}^{\text{DRX}} = \sum_{a_k}\sum_{b_k}\sum_{c_k} a_k \left(\frac{-\theta}{\rho}\right)^{b_k} \times \frac{d^{b_k}}{ds^{b_k}}\left(\mathcal{L}_{I_{\text{CUE}}^{\text{DRX}}}(s)\mathcal{L}_{I_{\text{DTX}}^{\text{DRX}}}(s)\right)\Big|_{s=c_k\frac{\theta}{\rho}}, \quad (12)$$

where $\{a_k\}$, $\{b_k\}$ and $\{c_k\}$ are coefficients which can be derived using (23), $\frac{d^{b_k}}{ds^{b_k}}$ is the b_k-th order derivative with respect to s, $\mathcal{L}_{I_{\text{CUE}}^{\text{DRX}}}(s)$ and $\mathcal{L}_{I_{\text{DTX}}^{\text{DRX}}}(s)$ are the Laplace transform of the distribution of $I_{\text{CUE}}^{\text{DRX}}$ and $I_{\text{DTX}}^{\text{DRX}}$, respectively, which are given in Lemmas 4 and 5.

Proof: See Appendix B. ■

We illustrate the result of Theorem 2 for two important cases below.

Case 1: For the case where DTXs have a single antenna and DRXs have M_r antennas, the outage probability experienced at a typical DRX is given by

$$P_{\text{out}}^{\text{DRX}} = 1 - \sum_{k=0}^{M_r-1} \frac{(-s)^k}{k!}\frac{d^k}{ds^k}\left(\mathcal{L}_{I_{\text{CUE}}^{\text{DRX}}}(s)\mathcal{L}_{I_{\text{DTX}}^{\text{DRX}}}(s)\right)\Big|_{s=\frac{\theta}{\rho}}. \quad (13)$$

Note the k-th derivative of $\mathcal{L}_{I_{\text{CUE}}^{\text{DRX}}}(s)\mathcal{L}_{I_{\text{DTX}}^{\text{DRX}}}(s)$ is given by [20]

$$\frac{d^k}{ds^k}\left(\mathcal{L}_{I_{\text{CUE}}^{\text{DRX}}}(s)\mathcal{L}_{I_{\text{DTX}}^{\text{DRX}}}(s)\right) = \frac{\sum k! \exp(g(s))}{p_1!p_2!\ldots p_k!} \times \left(\frac{\frac{d}{ds}g(s)}{1!}\right)^{p_1}\left(\frac{\frac{d^2}{ds^2}g(s)}{2!}\right)^{p_2}\cdots\left(\frac{\frac{d^k}{ds^k}g(s)}{k!}\right)^{p_k}, \quad (14)$$

where the sum is over all non-negative integer solution of the Diophantine equation $p_1 + 2p_2 + \ldots kp_k = k$ and

$$g(s) = -(a+b)s^{\frac{2}{\eta_d}}, \quad (15)$$

$$\frac{d^k}{ds^k}g(s) = -(a+b)\prod_{i=0}^{k-1}\left(\frac{2}{\eta_d} - i\right)s^{\frac{2}{\eta_d}-k}, \quad (16)$$

$$a = \frac{2\pi\lambda_b}{\eta_d} E_{P_c}\left[P_c^{\frac{2}{\eta_d}}\right]\Gamma\left(\frac{2}{\eta_d}\right)\Gamma\left(1 - \frac{2}{\eta_d}\right), \quad (17)$$

$$b = \frac{2\pi P_{\text{D2D}}\lambda_d}{\eta_d} E_{P_d}\left[P_d^{\frac{2}{\eta_d}}\right]\Gamma\left(\frac{2}{\eta_d}\right)\Gamma\left(1 - \frac{2}{\eta_d}\right). \quad (18)$$

Proof: Using the fact that the cumulative distribution function (cdf) of the fading gain on the typical link follows the gamma distribution, we have $f_{g_0^{\text{DRX}}}(g_0^{\text{DRX}}) = 1 - \sum_{k=0}^{M_r-1}\frac{1}{k!}(g_0^{\text{DRX}})^k \exp(-g_0^{\text{DRX}})$. Then, combining it with Theorem 2 and Lemmas 4 and 5 and simplifying, we obtain the final result. ■

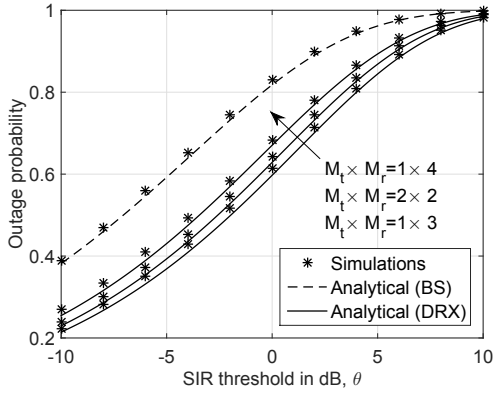

Fig. 1. Outage probability at the BS and DRX versus the SIR threshold θ.

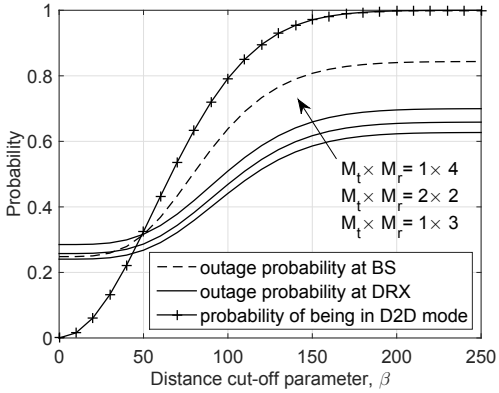

Fig. 2. Outage probability at the BS and DRX, and P_{D2D} versus the distance cut-off threshold β.

Case 2: For the case where both DTX and DRX have 2 antennas each, the outage probability experienced at a typical DRX is given by

$$P_{\mathrm{out}}^{\mathrm{DRX}} = 1 + \exp\Big(-(a+b)(2s)^{\frac{2}{\eta_d}}\Big) - 2\exp\Big(-(a+b)s^{\frac{2}{\eta_d}}\Big) - s^2\left(\frac{-2(a+b)\exp\left(-(a+b)s^{\frac{2}{\eta_d}}\right)\left(\frac{2}{\eta_d}-1\right)s^{\frac{2}{\eta_d}-2}}{\eta_d}\right) \times \exp\left(-(a+b)s^{\frac{2}{\eta_d}}\right) \times \left(\frac{-2(a+b)s^{\frac{2}{\eta_d}-1}}{\eta_d}\right)^2, \quad (19)$$

where $s = \frac{\theta}{\rho}$, a and b are given in (17) and (18), respectively.

Proof: Under this case, the CDF of g_0^{DRX} is given by $f_{g_0^{\mathrm{DRX}}}(g_0^{\mathrm{DRX}}) = 2\exp(-g_0^{\mathrm{DRX}}) - \exp(-2g_0^{\mathrm{DRX}}) + (g_0^{\mathrm{DRX}})^2\exp(-g_0^{\mathrm{DRX}})$. Combining it with Theorem 2 and Lemmas 4 and 5 and simplifying, we obtain the final result. ■

IV. Results

In this section, the accuracy of the outage probability results and the performance effects of the multiple antennas at D2D users are investigated through numerical evaluations. The parameters used in this section are as follows. The BS's density is set to $\lambda_b = 5$ BSs/km^2, the potential DTX's density is $\lambda_d = 50$ TXs/km^2. The maximum transmit power is set to $P_u = 0$ dB, the channel inversion received power is set to $\rho = -100$ dB, the path loss exponents of the cellular link and the D2D link are set to $\eta_c = \eta_d = 4$. The parametric values for $R_{\max}$ is derived using the equations $R_{\max} = \left(\frac{P_u}{\rho}\right)^{\frac{1}{\eta_d}}$.

A. Validation

Fig. 1 plots the outage probability at the BS and DRX versus the SIR threshold θ, for distance cut-off threshold $\beta = R_{\max}/2$, with different number of antennas at the DTX and DRX. The simulation results are generated using Matlab by averaging over 10^5 Monte carlo simulation runs. From Fig. 1, we can see that the analytical curves match closely with the simulation results (the difference is less than 5%). This validates our derived analytical results.

Fig. 1 shows that, regardless of the number of antennas at the DTX, the outage probability at the BS stays the same. This is in accordance with the explanation provided in Remark 1. For the outage probability at the DRX, comparing with the benchmark case of $M_t \times M_r = 1 \times 1$ (which is the same as the outage probability at the BS), we can see that multiple antennas help to improve the performance.

B. Impact of Multi-antenna D2D Users

Fig. 1 also shows that the outage probability at the DRX is best for the case of $M_t \times M_r = 1 \times 4$. This is because $M_t \times M_r = 1 \times 4$ has a total number of 5 antennas, whereas $M_t \times M_r = 2 \times 2$ and $M_t \times M_r = 1 \times 3$ only have 4 antennas in total. This suggests that, in general, adding more antennas at D2D users can improve the D2D communication performance. Comparing the cases of $M_t \times M_r = 2 \times 2$ and $M_t \times M_r = 1 \times 3$, we can see that equal number of D2D transmit and receive antennas can provide better D2D communication performance.

C. Impact of Distance Cut-off Parameter

Fig. 2 plots the outage probability at the BS and DRX, and the probability of being in D2D mode versus the distance cut-off threshold, β, with different number of antennas at the DTX and DRX. The performance trends for different $M_t \times M_r$ cases are the same as in the previous figure.

From Fig. 2, we can see that the outage probability increases as the threshold β increases. This trend can be explained as follows. A larger value of β improves the probability of being in D2D mode, which implies that more potential DTXs are performing in D2D mode. It also increases the average transmit power for DTXs. As a result, more interference is generated by the DTXs which increases the outage probability.

Fig. 2 also shows that when β is in the range from 0 to a certain value (e.g., 30 under this scenario), the outage probability stays essentially unchanged. This is due to the fact that, when distance cut-off threshold is within this range, the number of interfering DTXs is small and the interference from CUEs governs the network performance. When β is larger than a certain value (e.g., 30 under this scenario),

the interference from DTXs plays the dominant role and the outage probability increases. This suggests that a smaller distance cut-off threshold, which allows a smaller number of closely located multi-antenna D2D users to communicate and results in less interference, is a good choice since it does not adversely impact the cellular network performance.

V. Conclusions

In this paper, we have studied the performance of underlaid multi-antenna D2D communication in uplink cellular networks, where distance cut-off mode selection scheme is adopted to manage the interference to the BSs. Using stochastic geometry, we have derived approximate yet accurate closed-form expressions for the outage probability at the BS and D2D receiver. The results show that adding antennas at the D2D users does not impact the outage probability at the BS. In addition, equal number of D2D transmit and receive antennas can provide better D2D communication performance.

Appendix A
Proof of Theorem 1

Proof: Since the fading gain on the typical link follows the exponential distribution, we can rewrite as (7) as

$$\begin{aligned} P_{\text{out}} &= E_{I^{\text{BS}}_{\text{CUE}}, I^{\text{BS}}_{\text{DTX}}}\left[1-\exp\left(-\frac{\theta}{\rho}(I^{\text{BS}}_{\text{CUE}}+I^{\text{BS}}_{\text{DTX}})\right)\right] \\ &= 1 - E_{I^{\text{BS}}_{\text{CUE}}}\left[\exp\left(-\frac{\theta}{\rho}I^{\text{BS}}_{\text{CUE}}\right)\right] E_{I^{\text{BS}}_{\text{DTX}}}\left[\exp\left(-\frac{\theta}{\rho}I^{\text{BS}}_{\text{DTX}}\right)\right] \\ &= 1 - \left(\mathcal{L}_{I^{\text{BS}}_{\text{CUE}}}(s)\mathcal{L}_{I^{\text{BS}}_{\text{DTX}}}(s)\right)\Big|_{s=\frac{\theta}{\rho}}, \end{aligned} \tag{20}$$

where the last step comes from the fact that the Laplace transform of the pdf of a random variable z is $\mathcal{L}_z(s) = E_z[\exp(-sz)]$, $\mathcal{L}_{I^{\text{BS}}_{\text{CUE}}}(s)$ and $\mathcal{L}_{I^{\text{BS}}_{\text{DTX}}}(s)$ are the Laplace transform of the pdf of $I^{\text{BS}}_{\text{CUE}}$ and $I^{\text{BS}}_{\text{DTX}}$, respectively. In the following, we are going to derive these two quantities.

In general, the location of the interfering CUEs, ϕ'_c, does not following the PPP. However, in our system model only one CUE per cell generates the interference to the typical BS. Hence, for analytical tractability, we still approximate their locations as the PPP with density λ_b. Based on the probability generating functional for the PPP, we have the Laplace transform of the pdf of $I^{\text{BS}}_{\text{CUE}}$ as

$$\begin{aligned} \mathcal{L}_{I^{\text{BS}}_{\text{CUE}}}(s) &= E_{P_{ci},\phi'_c,g_i^{\text{BS}}}\left[\exp\left(-s\sum\nolimits_{x_i\in\phi'_c} P_{ci}|x_i|^{-\eta_c} g_i^{\text{BS}}\right)\right] \\ &= \exp\left(-\int_R^\infty E_{P_c,g^{\text{BS}}}\left[1-\exp((-sP_c g^{\text{BS}} r^{-\eta_c})\right] 2\pi\lambda_b r\mathrm{d}r\right) \\ &= \exp\left(-2\pi\lambda_b E_{P_c}\left[\int_R^\infty\left(1-\frac{1}{1+sP_c r^{-\eta_c}}\right) r dr\right]\right) \\ &= \exp\left(-2\pi\lambda_b E_{P_c}\left[\int_R^\infty\left(\frac{sP_c}{r^{\eta_c}+sP_c}\right) r dr\right]\right) \\ &= \exp\left(-2\pi\lambda_b E_{P_c}\left[\frac{{}_2F_1\left(1,1-\frac{2}{\eta_c};2-\frac{2}{\eta_c};-sP_cR^{-\eta_c}\right)}{(sP_cR^{2-\eta_c})^{-1}(\eta_c-2)}\right]\right) \\ &= \exp\left(-2\pi\lambda_b E_{r_c}\left[\frac{{}_2F_1\left(1,1-\frac{2}{\eta_c};2-\frac{2}{\eta_c};-s\rho r_c^{\eta_c}R^{-\eta_c}\right)}{(s\rho r_c^{\eta_c}R^{2-\eta_c})^{-1}(\eta_c-2)}\right]\right) \end{aligned}$$

$$\begin{aligned} &= \exp\Bigg(\frac{\pi\lambda_b R^2 s\rho}{(2-\eta_c)(2+\eta_c)} \\ &\quad\times\Bigg((2+\eta_c){}_2F_1\left(1,1-\frac{2}{\eta_c};2-\frac{2}{\eta_c};-s\rho\right) \\ &\quad+(2-\eta_c){}_2F_1\left(1,1+\frac{2}{\eta_c};2+\frac{2}{\eta_c};-s\rho\right)\Bigg)\Bigg). \end{aligned} \tag{21}$$

Note that in the second step we drop the index i since both the fading and the distance to the BS are identically and independent distributed. Additionally, the lower limit in the integral is R, instead of 0, since the closest distance between the CUE and the BS is R. The third step comes from the fact that the fading gain on the interfering link follows the exponential distribution.

The location of the interfering DTXs, ϕ'_d, follows the PPP with density $P_{\text{D2D}}\lambda_d$. Since the potential DTX being in D2D mode or not is an independent process, according to the thinning theorem [21], the resulting process is still PPP. Similar to the above derivation, we have the Laplace transform of the pdf of $I^{\text{BS}}_{\text{DTX}}$ given by

$$\begin{aligned} \mathcal{L}_{I^{\text{BS}}_{\text{DTX}}}(s) &= E_{P_{dj},\phi'_d,h_j^{\text{BS}}}\left[\exp\left(-s\sum\nolimits_{y_j\in\phi'_d} P_{dj}|y_j|^{-\eta_c} h_j^{\text{BS}}\right)\right] \\ &= \exp\Bigg(-2\pi P_{\text{D2D}}\lambda_d \\ &\quad\times E_{P_d,h^{\text{BS}}}\left[\int_0^\infty(1-\exp(-sP_d h^{\text{BS}} r^{-\eta_c}))r\mathrm{d}r\right]\Bigg) \\ &= \exp\left(-2\pi P_{\text{D2D}}\lambda_d E_{P_d}\left[\frac{P_d^{\frac{2}{\eta_c}} s^{\frac{2}{\eta_c}}}{\eta_c}\Gamma\left(\frac{2}{\eta_c}\right)\Gamma\left(1-\frac{2}{\eta_c}\right)\right]\right) \\ &= \exp\left(\frac{-2\pi P_{\text{D2D}}\lambda_d}{\eta_c} s^{\frac{2}{\eta_c}} E_{P_d}\left[P_d^{\frac{2}{\eta_c}}\right]\Gamma\left(\frac{2}{\eta_c}\right)\Gamma\left(1-\frac{2}{\eta_c}\right)\right), \end{aligned} \tag{22}$$

where $E_{P_d}\left[P_d^{\frac{2}{\eta_c}}\right]$ can be obtained using Lemma 3 and P_{D2D} is given in Lemma 1.

Combining the above two Laplace transforms and substituting (20), we obtain the result in Theorem 1. ■

APPENDIX B
PROOF OF THEOREM 2

Proof: Using the result in [22], the cdf of the fading gain on the desired D2D link is

$$F_{g_0^{\mathrm{DRX}}}(g_0^{\mathrm{DRX}}) = \frac{|\Psi(g_0^{\mathrm{DRX}})|}{\prod_{k=1}^{q}\Gamma(q-k+1)\Gamma(t-k+1)}, \quad (23)$$

where $|\cdot|$ denotes the determinant, $q = \min\{M_t, M_r\}$, $t = \max\{M_t, M_r\}$. The entries of the $q \times q$ matrix $\Psi(g_0^{\mathrm{DRX}})$ are

$$\{\Psi(g_0^{\mathrm{DRX}})\}_{i,j} = (t-q+i+j-2)! \times \left(1 - \exp(-g_0^{\mathrm{DRX}}) \sum_{k=0}^{t-q+i+j-2} \frac{(g_0^{\mathrm{DRX}})^k}{k!}\right), \quad (24)$$

where $i, j = 1, ..., q$.

Note that the above expression can be written as a sum-of-exponentials-and-polynomials form [11], i.e.,

$$F_{g_0^{\mathrm{DRX}}}(g_0^{\mathrm{DRX}}) = \sum_{a_k}\sum_{b_k}\sum_{c_k} a_k (g_0^{\mathrm{DRX}})^{b_k} \exp(-c_k g_0^{\mathrm{DRX}}). \quad (25)$$

To best of our knowledge, there is no explicit general form for coefficient sets $\{a_k\}$, $\{b_k\}$ and $\{c_k\}$. However, given the values of M_t and M_r, they can only be derived using (23). Substituting (23) into (9), we obtain the outage probability at the typical DRX as

$$\begin{aligned} P_{\mathrm{out}}^{\mathrm{D2D}} &= \Pr\left(g_0^{\mathrm{DRX}} < \frac{\theta}{\rho}\left(I_{\mathrm{CUE}}^{\mathrm{DRX}} + I_{\mathrm{DTX}}^{\mathrm{DRX}}\right)\right) \\ &= E_{I_{\mathrm{CUE}}^{\mathrm{DRX}}, I_{\mathrm{DTX}}^{\mathrm{DRX}}}\left[\sum_{a_k}\sum_{b_k}\sum_{c_k} a_k \left(\frac{\theta\left(I_{\mathrm{CUE}}^{\mathrm{DRX}} + I_{\mathrm{DTX}}^{\mathrm{DRX}}\right)}{\rho}\right)^{b_k} \right. \\ &\quad \left. \times \exp\left(-c_k \frac{\theta\left(I_{\mathrm{CUE}}^{\mathrm{DRX}} + I_{\mathrm{DTX}}^{\mathrm{DRX}}\right)}{\rho}\right)\right]. \end{aligned} \quad (26)$$

Using the fact that $\frac{d^{b_k}}{ds^{b_k}}\left(\exp\left(-s(I_{\mathrm{CUE}}^{\mathrm{DRX}} + I_{\mathrm{DTX}}^{\mathrm{DRX}})\right)\right) = (-1)^{b_k}(I_{\mathrm{CUE}}^{\mathrm{DRX}} + I_{\mathrm{DTX}}^{\mathrm{DRX}})^{b_k} \exp\left(-s(I_{\mathrm{CUE}}^{\mathrm{DRX}} + I_{\mathrm{DTX}}^{\mathrm{DRX}})\right)$, $\mathcal{L}_{I_{\mathrm{CUE}}^{\mathrm{DRX}}}(s)\mathcal{L}_{I_{\mathrm{DTX}}^{\mathrm{DRX}}}(s) = E_{I_{\mathrm{CUE}}^{\mathrm{DRX}}, I_{\mathrm{DTX}}^{\mathrm{DRX}}}[\exp(-s(I_{\mathrm{CUE}}^{\mathrm{DRX}} + I_{\mathrm{DTX}}^{\mathrm{DRX}}))]$, we obtain the result in Theorem 2. ■

REFERENCES

[1] A. Asadi, Q. Wang, and V. Mancuso, "A survey on device-to-device communication in cellular networks," *IEEE Commun. Surveys Tuts*, vol. 16, no. 4, pp. 1801–1819, Nov. 2014.

[2] F. Boccardi, R. W. Heath, A. Lozano, T. L. Marzetta, and P. Popovski, "Five disruptive technology directions for 5G," *IEEE Commun. Mag.*, vol. 52, no. 2, pp. 74–80, Feb. 2014.

[3] A. Orsino, M. Gapeyenko, L. Militano, D. Moltchanov, S. Andreev, Y. Koucheryavy, and G. Araniti, "Assisted handover based on device-to-device communications in 3GPP LTE systems," in *Proc. IEEE Globecom Workshops*, Dec. 2015.

[4] X. Lin, J. G. Andrews, and A. Ghosh, "Spectrum sharing for device-to-device communication in cellular networks," *IEEE Trans. Wireless Commun.*, vol. 13, no. 12, pp. 6727–6740, Dec. 2014.

[5] H. ElSawy, E. Hossain, and M.-S. Alouini, "Analytical modeling of mode selection and power control for underlay D2D communication in cellular networks," *IEEE Trans. Commun.*, vol. 62, no. 11, pp. 4147–4161, Nov. 2014.

[6] D. Marshall, S. Durrani, J. Guo, and N. Yang, "Performance comparison of device-to-device mode selection schemes," in *Proc. IEEE PIMRC*, Aug. 2015, pp. 1536–1541.

[7] M. Peng, Y. Li, T. Q. S. Quek, and C. Wang, "Device-to-device underlaid cellular networks under Rician fading channels," *IEEE Trans. Wireless Commun.*, vol. 13, no. 8, pp. 4247–4259, Aug. 2014.

[8] M. G. Khoshkholgh, Y. Zhang, K.-C. Chen, K. G. Shin, and S. Gjessing, "Connectivity of cognitive device-to-device communications underlying cellular networks," *IEEE J. Sel. Areas Commun.*, vol. 33, no. 1, pp. 81–99, Jan. 2015.

[9] G. George, R. K. Mungara, and A. Lozano, "An analytical framework for device-to-device communication in cellular networks," *IEEE Trans. Wireless Commun.*, vol. 14, no. 11, pp. 6297–6310, Nov. 2015.

[10] J. Guo, S. Durrani, X. Zhou, and H. Yanikomeroglu, "Device-to-device communication underlaying a finite cellular network region," 2015, submitted. [Online]. Available: http://arxiv.org/abs/1510.03162

[11] A. M. Hunter, J. G. Andrews, and S. Weber, "Transmission capacity of ad hoc networks with spatial diversity," *IEEE Trans. Commun.*, vol. 7, no. 12, pp. 5058–5071, Dec. 2008.

[12] M. D. Renzo, C. Merola, A. Guidotti, F. Santucci, and G. E. Corazza, "Error performance of multi-antenna receivers in a Poisson field of interferers: A stochastic geometry approach," *IEEE Trans. Commun.*, vol. 61, no. 5, pp. 2025–2047, May 2013.

[13] J. Zhang and J. G. Andrews, "Distributed antenna systems with randomness," *IEEE Trans. Commun.*, vol. 7, no. 9, pp. 3636–3646, Sep. 2008.

[14] J. G. Andrews, R. K. Ganti, M. Haenggi, N. Jindal, and S. Weber, "A primer on spatial modeling and analysis in wireless networks," *IEEE Commun. Mag*, vol. 48, no. 11, pp. 156–163, Nov. 2010.

[15] H. Min, J. Lee, S. Park, and D. Hong, "Capacity enhancement using an interference limited area for device-to-device uplink underlaying cellular networks," *IEEE Trans. Wireless Commun*, vol. 10, no. 12, pp. 3995–4000, Dec. 2011.

[16] S. Shalmashi, E. Björnson, S. Ben Slimane, and M. Debbah, "Closed-form optimality characterization of network-assisted device-to-device communications," in *Proc. IEEE WCNC*, Apr. 2014, pp. 508–513.

[17] A. Tolli, J. Kaleva, and P. Komulainen, "Mode selection and transceiver design for rate maximization in underlay D2D MIMO systems," in *Proc. IEEE ICC*, Jun. 2015, pp. 4822–4827.

[18] S. Shalmashi, E. Björnson, M. Kountouris, K. W. Sung, and M. Debbah, "Energy efficiency and sum rate when massive MIMO meets device-to-device communication," in *Proc. IEEE ICC*, Jun. 2015, pp. 627–632.

[19] A. Agarwal, S. Mukherjee, and S. K. Mohammed, "Impact of underlaid multi-antenna D2D on cellular downlink users in massive MIMO systems," *ArXiv Technical Report*, 2015. [Online]. Available: http://arxiv.org/abs/1511.00781

[20] X. Zhou, J. Guo, S. Durrani, and I. Krikidis, "Performance of maximum ratio transmission in ad hoc networks with SWIPT," *IEEE Wireless Communications Letters*, vol. 4, no. 5, pp. 529–532, Oct. 2015.

[21] M. Haenggi, *Stochastic Geometry for Wireless Networks*, ser. Wireless Communications. Cambridge University Press, Oct. 2012.

[22] M. Kang and M.-S. Alouini, "Largest eigenvalue of complex wishart matrices and performance analysis of MIMO MRC systems," *IEEE J. Sel. Areas Commun.*, vol. 21, no. 3, pp. 418–426, Apr. 2003.